DOI: 10.1002/cctc.201200017

Simultaneous Generation of Mesoxalic Acid and Electricity from Glycerol on a Gold Anode Catalyst in Anion-Exchange Membrane Fuel Cells

Le Xin, Zhiyong Zhang, Zhichao Wang, and Wenzhen Li*[a]

We report the selective electrocatalytic oxidation of glycerol for the cogeneration of mesoxalic acid and electricity on a gold anode catalyst in anion-exchange membrane fuel cells (AEMFCs). Small Au nanoparticles (3.5 nm) were uniformly deposited onto carbon black with a loading of 40 wt% through a solution-phase method. An AEMFC with this Au/C anode catalyst, together with an Fe-based cathode catalyst, exhibited a peak power density of 57.9 mW cm^{-2} at 80 °C. Valuable mesoxalic acid was produced with high selectivity (46%) from the electro-oxidation of glycerol on Au/C at an operating voltage of 0.3 V, whilst very small amounts of mesoxalic acid (selectivity < 3%) were obtained on a Pt/C anode catalyst in AEMFCs. The product distribution was dependent on the anode overpotential. At 1.2 V versus the standard hydrogen electrode (SHE) in an electrolysis cell, glycolic acid was the major product (selectivity: 65%) and no mesoxalic acid was observed. Based on the product analysis, we found that Au facilitated deeper-oxidation of glycerol to afford the fully-oxidized C_3 mesoxalic acid, rather than C–C cleavage, under a mild potential range (0.4–0.7 V vs. SHE) that was fortunately within the working voltage range of the fuel cells.

Introduction

Biomass is an intriguing renewable and carbon-neutral resource, and is expected to play a big part in the future energy landscape.[1] Glycerol is mass-produced as a low-value by-product (0.3 US$ kg^{-1}) in the manufacturing of biodiesel. Glycerol is a highly functionalized molecule that has great potential in the construction of major building blocks for the production of new polymers, fine chemicals, pharmaceuticals, etc.[2] The selective catalytic oxidation of glycerol by using molecular oxygen in aqueous-phase catalytic systems under moderate conditions (e.g., 20–80 °C, 3–10 bar) is a very attractive sustainable process owing to its low environmental impact, especially when compared to costly and non-environmentally friendly stoichiometric-oxidation processes.[2b,c,3] Glycerol contains one secondary- and two primary hydroxyl (OH) groups; the partial oxidation of glycerol can lead to the formation of several higher-value oxygenated chemicals, such as glyceric acid, tartronic acid, and mesoxalic acid. Among these compounds, mesoxalic acid (140 US$ g^{-1}) has potential applications as a complexing agent and as a precursor in the synthesis of 4-chlorophenylhydrazoned mesoxalic acid, which has been demonstrated to be an anti-HIV agent;[4] moreover, its salt form (i.e., potassium mesoxalate) has found applications in the treatment of diabetes.[2c]

Au catalysis have emerged as one of the most-exciting research areas in chemistry.[3e,h] The aqueous-phase oxidation of glycerol by using molecular oxygen has been extensively studied over Au[3c,5] and its bimetallic alloys, such as AuPt[6] and AuPd.[7] Au has demonstrated a unique ability to enhance the selective formation of glyceric acid from glycerol, that is, Hutchings and co-workers reported 100% selectivity and 54~56% conversion of glycerol under optimized alkaline conditions.[3c,5c,d] Ketchie et al. found that the presence of hydroxyl ions was required for the oxidation of glycerol over supported Au particles.[5b] They also observed that the presence of H_2O_2 as an oxidant improved the selectivity for glycolic acid, as opposed to glyceric acid, which was preferred in the presence of O_2. The influence of the Au-particle size has been investigated separately by several groups.[5a] Small Au particles were found to have a higher initial activity, but were not able to maintain the selectivity towards glyceric acid during the glycerol-oxidation reaction. Conversely, larger Au particles were less active but had a higher and more-stable selectivity for glyceric acid throughout the oxidation process.[5e] Until now, the predominant products from direct glycerol oxidation on Au catalysts in the aqueous alkaline phase have been glyceric acid[3c,g] and glycolic acid,[8] whereas the selectivity for tartronic acid has typically been < 15% and no mesoxalic acid has been reported.[2c]

Recently, based on DFT calculations and HPLC/MS isotope analysis, Davis and co-workers elegantly revealed that the presence of OH^- ions would greatly reduce the activation energy of the first dehydrogenation step, thereby facilitating glycerol oxidation.[3g] They inferred that O_2 merely facilitates the OH^--

[a] L. Xin,[+] Z. Zhang,[+] Z. Wang, Prof. W. Li
Chemical Engineering Department
Michigan Technological University
1400 Townsend Drive, Houghton, MI 49931 (USA)
Fax: (+1) 906-487-3213
E-mail: wzli@mtu.edu

[+] These authors contributed equally to this work.

Supporting information for this article is available on the WWW under http://dx.doi.org/10.1002/cctc.201200017.

regeneration loop, and that its function is similar to that in the oxygen-reduction reaction (ORR) at the cathode of a fuel cell. Because the glycerol reaction in the aqueous phase is a redox reaction in heterogeneous systems, and because O_2 functions in the same way as in the ORR in fuel cells, the study of electrocatalytic oxidation could provide new insights into heterogeneous catalytic oxidation reactions. Indeed, the electro-oxidation of glycerol over a polycrystalline Au electrode has been widely studied in three-electrode cells. FTIR[9] and HPLC[10] have been used to elucidate the mechanisms of oxidation: FTIR spectroscopy has detected the presence of tartronic acid, glyoxylic acid, and mesoxalic acid on an Au electrode surface at high potentials [>1.2 V vs. standard hydrogen electrode (SHE)].[9b] However, FTIR merely probes the instant adsorbates or intermediates that are formed during glycerol oxidation. To detect the presence of any stable products in the liquid electrolyte, HPLC is a more-straightforward tool. The most-abundant product from the electro-oxidation of glycerol on a polycrystalline Au electrode in alkaline media, as examined by HPLC, is glyceric acid at low potentials (0.6–0.8 V), and glycolic acid at high potentials (0.8–1.5 V).[10a,c]

Glycerol has been considered as a potential fuel for direct alcohol fuel cells (DAFC), owing to its relatively low price, simple purification and storage, as well as its non-volatile and environmentally friendly properties.[11] Pt- and Pd-based anode catalysts have been investigated in anion-exchange membrane direct glycerol fuel cells (AEM-DGFCs), and considerably high fuel-cell-output power densities have been achieved (125 mW cm^{-2} on Pt/C[11c] and 120 mW cm^{-2} on PdNiZn/C[11b]) However, because Au has exhibited higher onset potentials for glycerol oxidation in three-electrode-cell studies, it inevitably leads to higher anode overpotential,[9a,10] and thus lower fuel-cell output power densities; thus, little work has been carried out on the application of Au anodes in AEM-DGFCs.

From energy conservation, economic, and sustainable chemistry viewpoints, the efficient cogeneration of electricity and valuable chemicals from glycerol at ambient temperature and pressure is highly desirable. Herein, carbon-supported Au nanoparticles (Au/C, 40 wt%) with an average particle diameter of 3.5 nm and a narrow size distribution (2–6 nm) were synthesized and used at the anode in an AEM-DGFC reactor with a non-platinum-group-metal cathode catalyst Fe-Cu-N_4/C (Fe-Cu-N-based macrocycle). The simultaneous generation of electricity and the synthesis of valuable chemicals were successfully achieved. The Au/C catalyst exhibited good performance for electricity generation (57.9 mW cm^{-2} at 80 °C) and demonstrated a unique catalytic selectivity towards mesoxalic acid (46%). The final product distribution was highly dependent on both the operating voltage of the fuel cell (anode overpotential) and on the Au/C catalyst (when compared with Pt/C). After assembling the Au/C catalyst into a self-designed electrolysis cell, we determined the relationship between product selectivity and anode overpotential and proposed a possible reaction pathway for the electro-oxidation of glycerol on Au/C in an AEM-DGFC reactor.

Results and Discussion

Characterizations of the catalysts

Au/C and Pt/C catalysts were prepared according a modified organic solution-phase-based nanocapsule procedure.[12] The X-ray diffraction (XRD) patterns (Figure 1a) indicated that both Pt/C and Au/C displayed face-centered-cubic (fcc) patterns. The average sizes of the Pt/C and Au/C metal crystals, as calculated by the Debye–Scherrer formula[12b] and based on the (220) diffraction peaks, were 1.9 nm and 2.7 nm, respectively. TEM images of Au/C and Pt/C (Figure 1b,d) showed that most of the nanoparticles were round in shape and were uniformly dispersed over the carbon support with minimal agglomeration. The histograms of particle size, which was counted from over 100 randomly chosen Au and Pt particles in arbitrary areas, showed narrow size distributions of 2–6 nm for Au/C (Figure 1c) and 1–4 nm for Pt/C (Figure 1d). The average particle sizes were 2.4 nm and 3.5 nm for Pt/C and Au/C, respectively, which were in good agreement with the XRD analysis. Comparing to previous studies,[5f] our self-prepared Au/C catalyst exhibited a smaller size and less agglomeration, thus indicating that this nanocapsule method was able to control the particle size and morphology of Au/C, even with a high metal loading of 40 wt%.

Efficient electricity generation from glycerol in AEM-DGFC

When applied as an AEM-DGFC anode catalyst, Au/C demonstrated high electricity-generation performance (Figure 2). With an Au loading of 1.0 mg cm^{-2}, the AEM-DGFC that was fed with 2.0 M KOH+1.0 M glycerol produced an open-circuit voltage (OCV) of 0.59 V and a peak power density of 17.5 mW cm^{-2} (at 110 mA cm^{-2}) at 50 °C. The performance was significantly improved on increasing the temperature to 80 °C: the OCV and maximum power density reached 0.67 V and 57.9 mW cm^{-2} (at 240 mA cm^{-2}), respectively. This increase was mainly due to greatly enhanced glycerol-oxidation kinetics at higher temperatures. The output power density of the Au/C anode AEM-DGFC was much higher than state-of-art biofuel cells that use glycerol fuel (typically <1.0 mW cm^{-2}).[13] Moreover, these results were competitive with current PtRu-anode-based proton-exchange membrane direct-methanol fuel cells (PEM-DMFCs), even with significantly lower precious-metal loading on the membrane electrode assembly (MEA; 1.0 $mg_{Au}\,cm^{-2}{}_{MEA}$ for AEM-DGFC versus >5.0 $mg_{Pt+PtRu}\,cm^{-2}{}_{MEA}$ for PEM-DMFC).[14] The high activity toward glycerol oxidation and promising AEMFC performance may have been due to the small Au nanoparticles (3.5 nm) with a narrow particle-size distribution (2–6 nm), which offered a high active surface area and a higher number of Au atoms at the edges (with higher intrinsic activity).[5a,d,e] However, with the same catalyst loading, the Pt/C anode AEM-DGFC exhibited an OCV of 0.80 V and a peak power density of 58.6 mW cm^{-2} at 50 °C, which were higher than that of the Au/C anode AEM-DGFC under the same conditions, thereby indicating that Au possessed an intrinsic catalytic activity that was lower than that of Pt. Our in-situ anode-po-

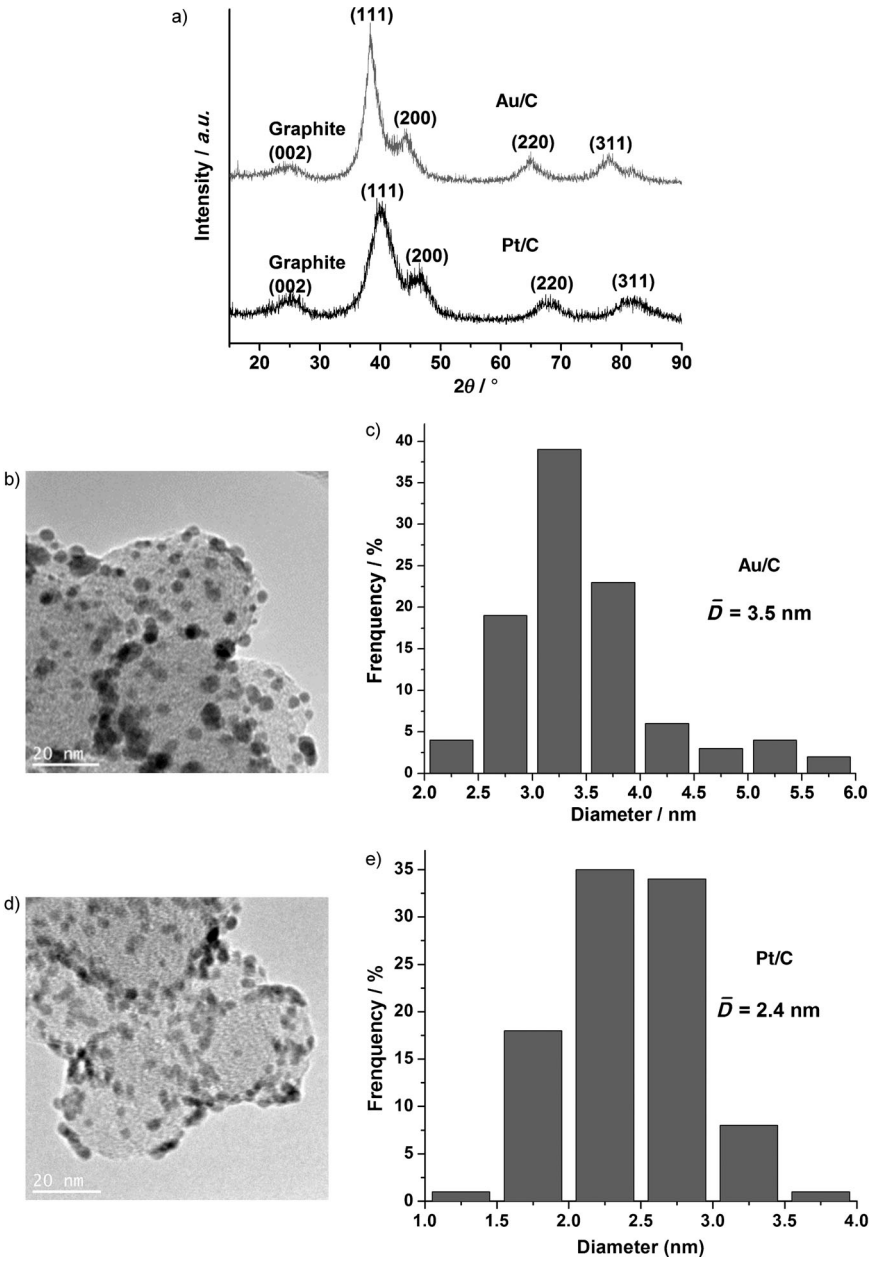

Figure 1. a) XRD patterns, b, d) TEM images, and c, e) particle-size histograms of the Au/C (b, c) and Pt/C (d, e) catalysts.

larization curves also showed about a 200 mV anode overpotential benefit by using Pt rather than Au at the OCV state (see the Supporting Information, Figure S1). This result was consistent with previous results in three-electrode cells: Although Au exhibited a higher current density than Pt at potentials of >0.85 V (vs. SHE), its onset potential was around 200 mV more positive than that on Pt.[9a]

Selective electrocatalytic oxidation of glycerol in an AEM-DGFC reactor

Table 1 shows the thermodynamic properties for the electro-oxidation of hydrogen and biorenewable alcohols (glycerol and EtOH). Chemical production did not necessarily come at the expense of electricity-generation efficiency. For example, the thermodynamic efficiency (η) and reversible potential (E_0) for the partial oxidation of glycerol into mesoxalic acid were 98.1% and 1.117 V, respectively, which were comparable to those for the complete oxidation of glycerol into CO_2 (combustion of glycerol, 98.4%, 1.230 V). During the oxidation of glycerol into mesoxalic acid, the volumetric energy density (W_e) of glycerol was 4.5 kW h L^{-1}, which was also close to that of the complete oxidation of glycerol into CO_2 (6.3 kW h L^{-1}). The Faradic efficiency (η_e), which is the ratio of transferred electrons in the partial oxidation to that in the complete oxidation (combustion of glycerol), was also high (71.4%, 10*e*:14*e*) for oxidizing glycerol into mesoxalic acid. Moreover, both the volumetric energy density and the Faradic efficiency for the partial oxidation of glycerol into mesoxalic acid were higher than those for the oxidation of ethanol (a biorenewable mono-alcohol) into acetic acid (2.1 kW h L^{-1}, 33.3%, 4*e*:12*e*), which was the most-abundant product in alkaline media. Therefore, it was theoretically feasible and practical to simultaneously generate higher-valued mesoxalic acid and electricity from the electro-oxidation of glycerol in

Table 1. Thermodynamic data of the electro-oxidation of biorenewable alcohols into target products.[15]

Fuel	Final product	N_e[a]	E_0[b] [V]	W_e[c] [kW h L^{-1}]	η_e[d] [%]	η[e] [%]
hydrogen	H_2O	2	1.229	2.6	100	83.3
ethanol	CO_2	12	1.145	6.4	100	96.9
	acetic acid	4	1.171	2.1	33.3	91.8
glycerol[f]	CO_2	14	1.230	6.3	100	98.4
	glyceric acid	4	1.140	1.8	28.6	91.1
	tartronic acid	8	1.170	3.6	57.1	98.4
	mesoxalic acid	10	1.117	4.5	71.4	98.1

[a] N_e: number of transferred electrons; [b] E_0: thermodynamic reversible potential; [c] W_e: volumetric energy density, liquid H_2; [d] η_e: Faradic efficiency; [e] η: thermodynamic efficiency; [f] based on predicted thermodynamic data from Ref. [16].

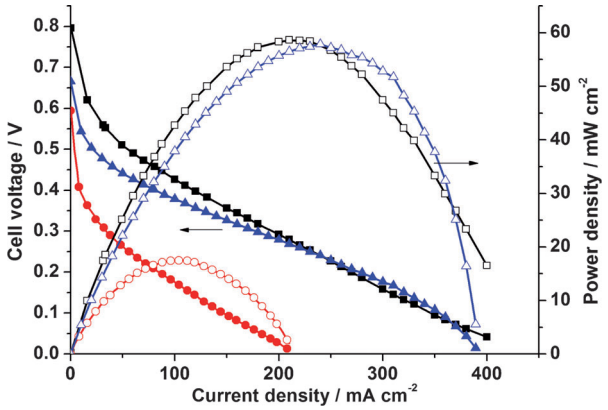

Figure 2. Polarization (filled symbols) and power-density curves (empty symbols) of AEM-DGFC with the Pt/C anode catalyst at 50 °C (■/□) and the Au/C catalyst at 50 °C (●/○) and at 80 °C (▲/△). Anode: Pt/C or Au/C, 1.0 $mg_{metal}\,cm^{-2}$, 2.0 M KOH+1.0 M glycerol, 4.0 mL min^{-1}. Cathode: Fe-Cu-N_4/C, 1.0 mg cm^{-2}, O_2, 400 mL min^{-1}, 30 psi.

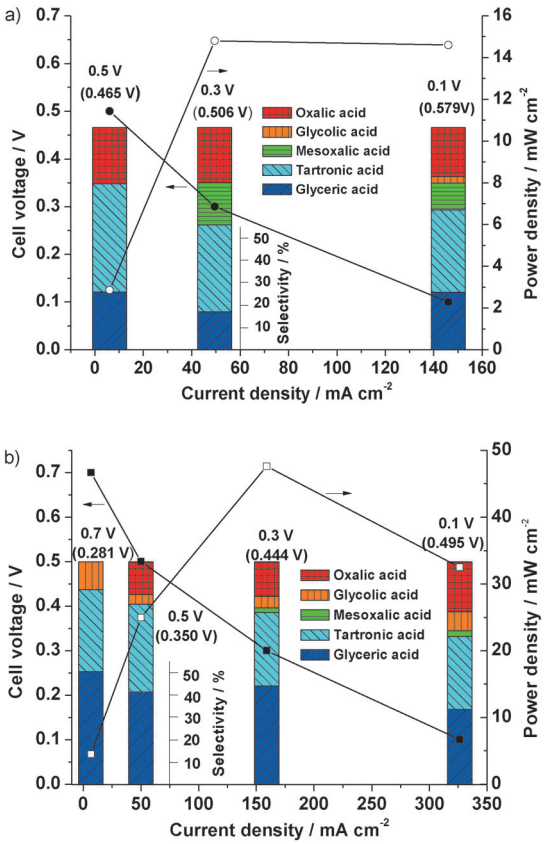

Figure 3. Product selectivity and the generation of electricity from the electrocatalytic oxidation of glycerol on a) Au/C and b) Pt/C with 2.0 M KOH+1.0 M glycerol in a single AEMFC reactor for 2 h at each operating voltage at 50 °C. The anode-catalyst loading was 1.0 $mg_{metal}\,cm^{-2}$. Anode overpotentials (vs. SHE) are given in parentheses.

AEM-DGFC, with little effect on electricity-generation efficiency.

Herein, the selective electrocatalytic oxidation of glycerol was conducted by continuously looping 2.0 M KOH+1.0 M glycerol (55 mL) from a plastic vessel into the anode compartment of an AEM-DGFC for 2 h. A constant fuel-cell voltage (0.5, 0.3, or 0.1 V) was applied by controlling the outer-circuit resistance and electricity was simultaneously generated. Figure 3a shows the glycerol-oxidation-product distribution and electricity-generation performance on an Au/C anode with a loading of 1.0 $mg_{Au}\,cm^{-2}$. During the oxidation, the average anode overpotentials were monitored by using an Hg/HgO electrode and the values (reported vs. SHE) are given in parentheses (Figure 3a) with their corresponding fuel-cell operating voltages. Figure 3a and Table 2 show that the selectivity for mesoxalic acid was controlled by the fuel-cell operating voltage (anode overpotentials): At 0.5 V, which was close to the open-circuit voltage, the anode overpotential was 0.465 V versus SHE, and no mesoxalic acid product was detected. Instead, selectivities of 26, 49, and 25% were obtained for glyceric acid, tartronic acid, and oxalic acid, respectively, with 3.5% glycerol conversion. When the fuel-cell operating voltage was decreased to 0.3 V, the anode overpotential increased to 0.506 V and mesoxalic acid was observed in the final mixture of products with a selectivity of 19% at 7.4% glycerol conversion. Moreover, electricity was generated with a peak power density of 14.8 mW cm^{-2}. The yield of mesoxalic acid seemed to suppress the selectivity for tartronic acid from 49% to 39%. When the fuel-cell voltage was decreased further to 0.1 V, which was sufficiently low to reach the limiting current density, the anode overpotential increased to 0.579 V and lower selectivity for mesoxalic acid (12%) was observed. Under the higher anode

Table 2. Electro-oxidation of glycerol on Au/C and Pt/C in AEM-DGFC at different fuel-cell operating voltages.[a]

Anode catalyst	Cell voltage [V]	Anode over-potential [V vs. SHE]	Selectivity[d] [%]					Glycerol conversion [%]	Carbon balance [%]	Power density [mW cm^{-2}]
			GA	TA	MA	GLA	OA			
Au/C[b]	0.5	0.465	26	49	0	0	25	3.5	0.43	2.9
	0.3	0.506	17	39	19	0	25	7.4	0.51	14.8
	0.1	0.579	26	37	12	3	22	20.0	0.78	14.6
Au/C[c]	0.5	0.448	13	32	28	0	27	3.2	1.2	5.7
	0.3	0.531	13	19	46	0	22	7.2	2.0	22.7
	0.1	0.633	14	22	34	0	30	12.5	0.4	13.8
Pt/C[b]	0.7	0.281	47	37	0	16	0	4.4	4.3	4.5
	0.5	0.350	41	40	0	4	15	10.5	6.5	25.0
	0.3	0.444	44	33	2	5	16	21.5	14.0	47.6
	0.1	0.495	34	33	3	8	22	37.5	26.1	32.5

[a] Reaction conditions: anode: 2.0 M KOH+1.0 M glycerol, 4.0 mL min^{-1}, cathode: Fe-Cu-N_4/C (Acta), 1.0 mg cm^{-2}, high-purity O_2 (99.999%), P_{O2} = 30 psi, 400 mL min^{-1}, 50 °C; [b] catalyst loading: 1.0 $mg_{metal}\,cm^{-2}$; [c] catalyst loading: 5.0 $mg_{Au}\,cm^{-2}$; [d] GA = glyceric acid, TA = tartronic acid, MA = mesoxalic acid, GLA = glycolic acid, OA = oxalic acid.

overpotential (0.579 V vs. SHE), glycerol conversion within 2 h jumped to 20% and a small amount of glycolic acid (3%) was formed. At a cell voltage of 0.1 V, the anode overpotential gradually increased during the reaction owing to the continuous consumption of glycerol, whereas, at higher fuel-cell operating voltages (0.5 and 0.3 V), the glycerol consumption was $<7.4\%$ and would not affect the anode overpotential. Thus, the anode overpotentials that were observed at higher cell voltages were quite stable with minor variations.

To further investigate the effects of reaction time, and the corresponding increase in anode overpotential, on mesoxalic selectivity, the reaction time was prolonged to 6 h. The same reaction conditions were used at the fuel-cell operating voltage of 0.1 V. The anode overpotential increased from 0.498 V at 30 min to 0.630 V over the 6 h reaction (see the Supporting Information, Figure S2 A). As a result, the initial selectivity for mesoxalic acid (22%) could not be maintained. The concentration of mesoxalic acid decreased after 2 h, thereby leading to the drop in selectivity (see the Supporting Information, Figure S2 B), whilst the concentrations of tartronic acid, glycolic acid, and oxalic acid gradually increased, with a corresponding increase in their selectivity. These results confirmed that the oxidation of glycerol into deeper-oxidized mesoxalic acid underwent a metal-surface-catalyzed step, as proposed by Davis and co-workers.[3g, 5b] In the electrocatalytic process, this step would be enhanced on a polarized Au surface. Herein, the degree of positive polarization on Au increased as the anode overpotential increased, which promoted the formation of tartronic acid from the oxidation of glyceric acid. Tartronic acid is a crucial intermediate that is directly oxidized into mesoxalic acid.[17] This process was favored within a mild anode overpotential range on Au/C. We suggested that the formation of mesoxalic acid was accompanied by its decarboxylation into oxalic acid, which could be accelerated at higher anode overpotentials. The accumulation of glycolic acid presumably resulted from the C–C bond cleavage of glyceric acid at higher anode overpotentials.

Our AEMFC electrocatalytic reactor could be envisioned as a continuous fixed-bed reactor with a series of multiple reactors. It was similar to the fixed-bed reactor for heterogonous catalysis, through which the yields of deeper-oxidized products, such as tartronic acid and oxalic acid, were enhanced on Au/C in high-pH environments.[18] However, our reactor had significant differences from heterogeneous catalytic reactors: 1) The anion-exchange membrane was introduced to separate the O_2 gas phase from the catalyst–electrolyte (solid–liquid) phase, to resolve the problem of oxygen mass transfer that was encountered by the multiphase reactor.[18a, 19] 2) The liquid-diffusion electrode was not only used as a catalyst bed but also as a conductor to collect electric current. Therefore, the cogeneration of electricity and higher-value chemicals could be achieved. 3) Large amounts of mesoxalic acid were selectively produced by using the electrocatalytic reactor with an Au/C-anode catalyst. To the best of our knowledge, mesoxalic acid has never been synthesized with high selectivity from the direct catalytic oxidation of glycerol on metal catalysts in high pH environments, and it was only detected on the Au electrode surface at very high potentials (>1.2 V vs. SHE) in alkaline media by using in situ FTIR spectroscopy.[9b]

In sharp contrast to Au/C, Pt/C was more active for the electro-oxidation of glycerol under the AEM-DGFC operating conditions, as shown by its larger peak power density, lower anode overpotential, and higher glycerol conversion (Figure 3 b, Table 2). Owing to the strong interactions between the Pt/C catalyst surface and the hydroxyl- and oxygenated functional groups, the C–C bond was easier to break over the Pt/C anode catalyst in AEM-DGFCs. Only a small amount of mesoxalic acid (2–3%) was collected at cell voltages below 0.3 V, and the formation of C_2 products occurred in a much-lower anode-overpotential region on Pt/C than on the Au/C anode catalyst, that is, the yields of glycolic acid and oxalic acid occurred at anode overpotentials of 0.281 and 0.350 V versus SHE on Pt/C, respectively, compared to 0.579 and 0.465 V (vs. SHE) on Au/C. This phenomenon indicated that, on Pt/C, less energy (low potentials) was required for both glyceric acid and tartronic acid to break their C–C bonds rather than be further oxidized into mesoxalic acid. In addition, Table 2 shows the carbon balance, which was based on the detected C_2 and C_3 products, over the Pt/C and Au/C catalysts. When Pt/C was used as the anode catalyst, the carbon balance increased from 4.3% to 26.1% as the fuel-cell voltage decreased from 0.7 V to 0.1 V, whilst, at all of the investigated potentials on the Au/C anode catalyst, the carbon balance was typically $<1\%$, thus indicating that more C_2 products were further oxidized into C_1 products (formic acid and carbon dioxide) on Pt/C as compared to Au/C.

Interestingly, when the Au/C-anode loading was increased to 5.0 $mg_{Au}\,cm^{-2}$, considerably higher selectivity for mesoxalic acid (46% with a glycerol conversion of 7.2%) was obtained with an output peak power density of 22.7 $mW\,cm^{-2}$ at 0.3 V (Figure 4, Table 2). Glycerol conversions on both the Au-loaded anodes (1.0 $mg\,cm^{-2}$ and 5.0 $mg\,cm^{-2}$) were comparable at each cell voltage investigated; however, different product distributions were observed. Compared with the anode with 1.0 $mg_{Au}\,cm^{-2}$ loading, the selectivity for mesoxalic acid by

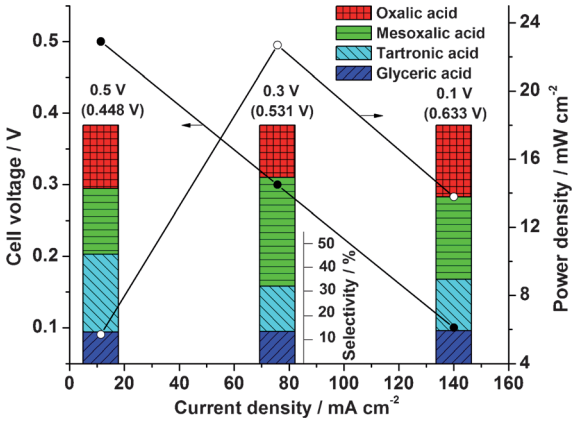

Figure 4. Product selectivity and the generation of electricity from the electrocatalytic oxidation of glycerol on an Au/C anode AEM-DGFC with 2.0 M KOH+1.0 M glycerol at each operation voltage for 2 h at 50 °C. The anode catalyst loading was 5.0 $mg_{Au}\,cm^{-2}$. Anode overpotentials (vs. SHE) are given in parentheses.

using the anode with 5.0 $mg_{Au}\,cm^{-2}$ loading increased significantly (from 0% to 28%) at 0.5 V, whilst the selectivity for tartronic acid dropped from 49% to 32%. As the cell potential was further lowered to 0.3 V, a significant amount of mesoxalic acid was produced with a selectivity of 46%, whilst the selectivity for tartronic acid dropped to 19%. These results indicated that the production of mesoxalic acid in this AEMFC reactor might follow a sequential oxidation process starting from glycerol, that is, glycerol→glyceric acid→tartronic acid→mesoxalic acid, which has been demonstrated in heterogeneous catalysis systems in low-pH media.[17,20] The selectivity of 46% for mesoxalic acid in the AEM-DGFC reactor indicated that the average selectivity of each reaction intermediate (glyceric acid, tartronic acid, and mesoxalic acid) should exceed 77%! However, further decreasing the cell potential to 0.1 V led to a decrease in the selectivity for mesoxalic acid, but an increase in the selectivity for oxalic acid. Compared to the anode with 1.0 $mg_{Au}\,cm^{-2}$ loading, no glycolic acid was observed with 5.0 $mg_{Au}\,cm^{-2}$ loading at the anode, which indicated that high Au loading (high ratio of catalyst to glycerol) favored the oxidation of the hydroxyl groups of the C_3 acids without breaking their C–C bonds. We also observed that the carbon balance remained within 2.0% (Table 2) by using the anode with 5.0 $mg_{Au}\,cm^{-2}$ loading, thereby suggesting that, despite large amounts of fully oxidized C_3 product (mesoxalic acid) being produced, negligible quantities of C_2 products were broken into C_1 products. The higher yield of mesoxalic acid would result in a higher Faradic efficiency of the fuel cell and greater utilization of glycerol fuel.

Stability test of the Au/C-anode AEM-DGFC reactor

The stability of the Au/C-anode AEM-DGFC reactor was investigated over 10 runs with an operation time of 2 h for glycerol oxidation with 2.0 M KOH+1.0 M glycerol under the same test conditions (Figure 5). The anode-catalyst loading was maintained at 5.0 $mg_{Au}\,cm^{-2}$, whilst the cathode-catalyst loading was increased to 2.0 $mg\,cm^{-2}$ to minimize the effect of the loss of catalytic activity. The fuel-cell operating voltage was fixed at 0.3 V, at which the Au/C anode AEM-DGFC generated the highest selectivity for mesoxalic acid, as well as the highest power density. After each run, the anode was cleaned by flushing with deionized water until the OCV was <0.01 V. The glycerol conversion and selectivity for mesoxalic acid increased to 10% and 49%, respectively, presumably owing to the increase in catalyst loading at the cathode (Figure 5). The selectivity for each product remained almost constant over the 10 runs, thereby indicating that the catalytic activity and selectivity on Au/C was stable over repeated cycles. Meanwhile, the Au/C anode also showed good stability against deactivation; the glycerol conversion stabilized at about 10% and the power density remained steady at about 27.6 $mW\,cm^{-2}$ (see the Supporting Information, Figure S3). The internal resistances during the reactions were stable at about 142 $mOhm\,cm^{-2}$ (see the Supporting Information, Figure S3), thus indicating that no structural changes of either the anode and cathode catalyst layers occurred, and no decomposition of the AEM occurred, even after 10 runs (a total operation time of 20 h).

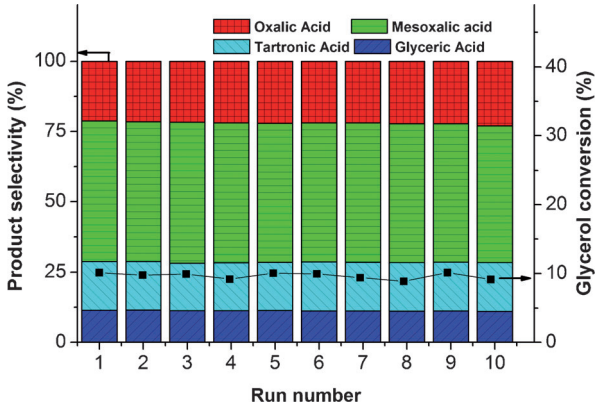

Figure 5. Stability of an Au/C anode AEM-DGFC with 2.0 M KOH+1.0 M glycerol at the fuel-cell operating voltage of 0.3 V at 50 °C; anode-catalyst loading: 5.0 $mg_{Au}\,cm^{-2}$; cathode-catalyst loading: 2.0 $mg\,cm^{-2}$

Potential-controlled selective electrocatalytic oxidation of glycerol in an AEM-based electrolysis cell

Although these AEMFC studies revealed a correlation between the anode overpotential and the selectivity for mesoxalic acid, two properties of the fuel cell hindered the accurate investigation of this relationship: 1) The anode overpotential in fuel cells was not directly controlled; it could only be monitored at various fuel-cell operating voltages. Moreover, at a lower cell voltage (about 0.1 V) at which glycerol reacted faster, the anode overpotential gradually increased owing to the continuous drop in fuel concentration. 2) Restricted by the theoretical AEM-DGFC voltage and the huge overpotential at the cathode, the anode overpotential was narrowed to a small region (0.4–0.7 V). The reaction and selectivity at higher anode overpotentials are still unclear.

To more-accurately study the effects of potential (more-stable- and more-controlled applied potential at the anode) on the selective electro-oxidation of glycerol and over a wider potential range, we assembled an electrolysis cell reactor with a carbon cloth diffusion-layer-supported Au anode (5.0 $mg_{Au}\,cm^{-2}$) and a Pt-based cathode (see the Supporting Information, Figure S4). The potential was accurately controlled from 0.4–1.2 V versus SHE by using a Hg/HgO electrode that was dipped into the anode compartment. Although the electro-oxidation of glycerol in alkaline media has already been reported on both a polycrystalline Au electrode and supported Au catalysts, most of these reports were only carried out in conventional three-electrode cells with diluted glycerol solution (0.1 M) and either a bulk Au electrode or a very small amount of Au nanoparticle catalyst that was deposited on a glassy carbon electrode.[9a,b,10] Owing to the low glycerol concentration and small electrochemical surface area of the Au/C catalyst, the reported onset potentials for the electro-oxidation of glycerol were as high as 0.55–0.65 V versus SHE, which were not consistent with the monitored anode overpotential at OCV of real AEM-DGFC (0.406 V in our tests, with an Au loading of

5.0 $mg_{Au}\,cm^{-2}$). On the other hand, the main products that were detected by HPLC were only glycolic acid and formic acid because C–C bond breakage was predominant at high applied potentials. The deeper-oxidized C_3 acids (i.e., tartronic acid and mesoxalic acid) were only detected at high potentials by using FTIR spectroscopy (>1.2 V vs. SHE). Compared with previous studies on the electro-oxidation of glycerol in traditional three-electrode cells, the electrolysis cell could be used to investigate the oxidation of glycerol at lower potentials, owing to the high catalyst loading (high ratio of catalyst to glycerol). Herein, stable anodic oxidation currents were obtained at 0.4 V versus SHE, which was close to the anode overpotential in AEM-DGFC at the OCV condition (0.406 V vs. SHE) with the same Au catalyst loading (5.0 $mg_{Au}\,cm^{-2}$).

After a reaction time of 30 min at each applied potential, the product distribution was analyzed by HPLC (Figure 6, Table 3). Interestingly, we observed an amazing consistency in the selectivities for the products between the electrolysis cell reactor and the fuel cell reactor. At 0.4 V versus SHE, the selectivity for glyceric acid, tartronic acid, and mesoxalic acid in the electrolysis cell were 15, 27, and 35%, respectively, which were in good agreement with the values that were obtained in a fuel cell with an Au catalyst of 5.0 $mg_{Au}\,cm^{-2}$ and a cell-operating voltage of 0.5 V (anode overpotential, 0.448 V vs. SHE): 13, 32, and 28%. As the anode overpotential increased, the selectivity for tartronic acid in both the electrolysis cell and the fuel cell gradually decreased to about 20%. The highest selectivity for mesoxalic acid (46%), which was obtained in a fuel cell with an operating voltage of 0.3 V (anode overpotential of 0.531 V), was also close to that obtained in an electrolysis cell at applied voltages of 0.5 V (47%) and 0.6 V (46%) at the anode.

Moreover, the electrolysis cell clearly exhibited a potential-controlled product distribution over a wider applied potential range than the fuel cell. At low potentials, the major product was mesoxalic acid. However, when the applied anode potential of the electrolysis cell was increased, the selectivity for C_2 acids (glycolic acid+glyoxylic acid+oxalic acid) increased gradually, thereby indicating that a higher overpotential facilitated the C–C bond breakage. When the applied anode potential was increased to 1.2 V, the predominant product was glycolic acid (65% selectivity), thus indicating that the glycerol-oxidation products were strongly dependent on the applied potential. The high selectivity for glycolic acid in the electrolysis cell reactor was in good agreement with previous studies in conventional three-electrode cells.[10a,c]

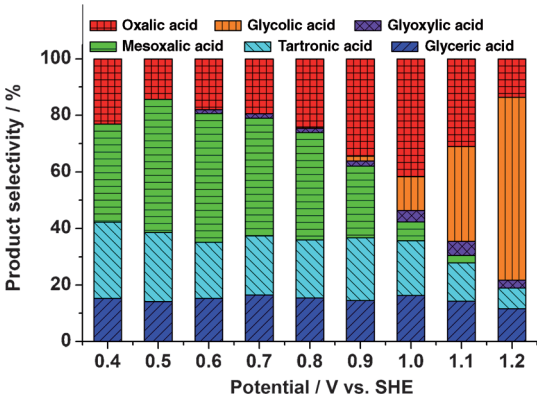

Figure 6. Selective electro-oxidation of glycerol on Au/C (5.0 $mg_{Au}\,cm^{-2}$) in an electrolysis cell under different applied potentials; reaction conditions: 2.0 M KOH+1.0 M glycerol, RT, reaction time: 0.5 h.

Table 3. Electro-oxidation of glycerol on Au/C in an electrolysis cell at different applied anode potentials.[a]

Applied anode potential [V vs. SHE]	Selectivity[b] [%]					
	GA	TA	MA	GLA	GLOA	OA
0.4	15	27	35	0	0	23
0.5	14	25	47	0	0	14
0.6	15	20	46	0	1	18
0.7	16	21	42	0	2	19
0.8	16	20	38	1	1	24
0.9	15	22	25	2	2	34
1.0	16	19	7	12	4	42
1.1	14	14	3	33	5	31
1.2	11	7	0	65	3	14

[a] The MEA for the electrolysis cell consisted of an Au/C anode (5.0 $mg_{Au}\,cm^{-2}$), a Pt/C cathode (1.0 $mg_{Pt}\,cm^{-2}$), and a solid anion-exchange membrane (FAA, 110 μm) with an active cross-sectional area of 1 cm^2. A Hg/HgO reference electrode in the anode chamber controlled the applied anode potential. Anode electrolyte: 2.0 M KOH+1.0 M glycerol (1.0 mL), cathode electrolyte: 2.0 M KOH (100 mL), RT. [b] GA = glyceric acid, TA = tartronic acid, MA = mesoxalic acid, GLA = glycolic acid, GLOA = glyoxylic acid, and OA = oxalic acid.

Reaction mechanism for the electrocatalytic oxidation of glycerol in an AEMFC reactor

Based on an analysis of the products in the bulk electrolyte in the fuel cell and in the electrolysis cell, we proposed a reaction pathway for the oxidation of glycerol (Scheme 1). The first step, that is, the oxidation of one primary hydroxyl group in glycerol to generate glyceric acid, was fast and started at 0.4 V

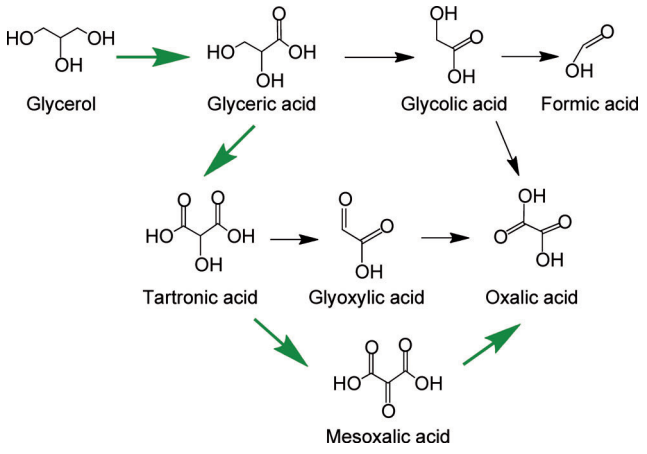

Scheme 1. Proposed reaction pathway for the electrocatalytic oxidation of glycerol on Au/C in a liquid-diffusion-electrode (LDE)–anion-exchange-membrane (AEM)-based electrolysis cell and fuel cell (green arrows represent the dominant pathways in a fuel cell).

versus SHE. As shown in Table 2 (AEM-DGFC reactor) and Table 3 (electrolysis cell reactor), with a catalyst loading of 5.0 $mg_{Au}\,cm^{-2}$, the selectivity for glyceric acid was stable at 11–16% over the whole potential range, thereby suggesting that it should be a stable reaction intermediate during the glycerol-oxidation reaction. This step was recently confirmed by using an online-sample collection, offline-HPLC analysis, in which glyceric acid was the first probed product at a relatively lower potential.[10a,c] However, because the reaction kinetics were greatly enhanced by the high ratio of catalyst to glycerol and high KOH concentrations, glyceric acid was rapidly oxidized into tartronic acid. As neither dihydroxyacetone nor hydroxypyruvic acid were detected over the whole voltage range for the fuel cell or the electrolysis cell, it was reasonable to believe that mesoxalic acid was produced through the direct oxidation of the hydroxyl group in tartronic acid. The C–C bond cleavage of mesoxalic acid gave oxalic acid at the low applied potential (or anode overpotential) of 0.4 V. In the fuel-cell operation, the anode overpotential was in the range 0.4–0.7 V; therefore, the detected oxidation products on the Au/C anode were glyceric acid, tartronic acid, mesoxalic acid, and oxalic acid. At a higher potential (0.6 V), tartronic acid began to be oxidized into glyoxylic acid, which could be further oxidized into oxalic acid. Although glycolic acid could be formed from tartronic acid through a non-Faradic decarboxylation pathway, we demonstrated that this reaction occurred in a non-oxidizing, low-pH environment.[8] Therefore, under these electrolysis conditions, glycolic acid was more likely to be converted from glyceric acid, which may have occurred at a relative higher potential (0.8 V), at which glycolic acid was observed in the electrolysis cell. This result was also consistent with the fuel-cell results: over the whole fuel-cell operating region (anode overpotential: 0.4–0.7 V vs. SHE), no glycolic acid was detected on the MEA with 5.0 $mg_{Au}\,cm^{-2}$ loading. To test whether the oxidation of glycolic acid led to the generation of glyoxylic acid, we investigated the electro-oxidation of glycolic acid (2.0 M KOH+0.5 M glycolic acid) under identical electrolysis reactor conditions (see the Supporting Information, Figure S5). Apart from the fact that, at a very high applied potential (1.2 V), glycolic acid was oxidized into formic acid with a selectivity of 50%, the only product from glycolic acid at lower potentials (0.7–1.1 V vs. SHE) was oxalic acid. Therefore, it was reasonable to conclude that glyoxylic acid in this system was mainly converted from the C–C cleavage of tartronic acid.

In summary, on the Au/C-based liquid-diffusion electrode: 1) it was easier to further oxidize the hydroxyl groups of the C_3 and C_2 acids (glyceric acid, tartronic acid, and glycolic acid) than to break their C–C bonds; 2) higher potential (energy) was needed to achieve deeper-oxidation and C–C bond cleavage of the C_2 acids than the C_3 acids. These insights into the electrocatalytic oxidation of glycerol will help the design of new Au-based electrocatalysts for the selective production of mesoxalic acid, that is, to facilitate the continuous hydroxyl-group oxidation of C_3 carboxylic acid, whilst avoiding their C–C bond cleavage.

Conclusions

We have demonstrated the efficient cogeneration of mesoxalic acid and electricity from the electro-oxidation of glycerol on small Au nanoparticles in an AEMFC reactor. A Au/C catalyst (40 wt%) with a small particle size (3.5 nm) and narrow particle-size distribution (2–6 nm) was prepared through a solution-phase reduction method. An AEMFC with the Au/C anode catalyst and a non-platinum-group-metal Fe-Cu-N_4/C cathode catalyst exhibited a peak power density of 57.9 $mW\,cm^{-2}$ at 80 °C. Valuable mesoxalic acid was directly produced with high selectivity (46%) from the electro-oxidation of glycerol under a fuel-cell working voltage of 0.3 V (the anode overpotential of 0.53 V vs. SHE) after 2 h. On the contrary, a very small yield of mesoxalic acid (selectivity $< 3\%$) was obtained on the Pt/C anode catalyst in the AEMFC operation. The oxidation-product distribution was also dependent on the fuel-cell operation voltage (anode overpotential). The selectivity towards mesoxalic acid decreased with increasing applied potential. At a high potential (1.2 V vs. SHE), glycolic acid was the major product with a selectivity of 65% and no mesoxalic acid was observed. Based on a product-distribution analysis in both fuel cells and electrolysis cells, Au facilitated the deeper oxidation of glycerol into the completely oxidized C_3 acid (mesoxalic acid), rather than C–C cleavage, under a mild potential range (0.4–0.7 V vs. SHE), which fortunately was within the working voltage range for the fuel cells.

Experimental Section

Preparation of Au/C

$AuCl_3$ (0.5 mmol, Acros Organics) was mixed with octadecene (16 mL, Acros Organics) and oleylamine (4 mL, Aldrich Chemistry) under a nitrogen blanket. The system was then rapidly heated to 80 °C, followed by a quick injection of $LiBEt_3H$ (1.5 mL, 1 M in THF, Acros Organics). After being maintained at the same temperature for 10 min, the solution was cooled to RT and separated by centrifugation. The as-prepared Au-NPs were deposited on Vulcan XC-72R carbon black (Cabot) to afford an Au/C catalyst with a loading of 40 wt% that was determined by inductively coupled plasma atomic emission spectroscopy (ICP-AES).

Preparation of Pt/C

$[Pt(acac)_2]$ (0.5 mmol, Acros Organics), oleylamine (200 μL, Aldrich Chemistry), and oleic acid (200 μL, Fisher Chemistry) were dissolved in a mixture of Vulcan XC-72R carbon black (Cabot) and benzyl ether (40 mL, Acros Organics, 99%) at 60 °C under a nitrogen blanket. $LiBEt_3H$ (1.0 mL, 1 M in THF, Acros Organics) was quickly injected into the system as the temperature was raised to 120 °C. After being maintained at 120 °C for 30 min, the temperature was slowly increased to 180 °C and maintained at that temperature for an additional 30 min. The Pt/C catalyst was collected by filtration, washed with copious amounts of EtOH, and dried in a vacuum oven overnight at 50 °C. The final metal loading of Pt/C was determined to be 40 wt% by ICP-AES.

Physicochemical characterization

The Au/C and Pt/C catalysts were characterized by TEM (JEOL 2010 with an operating voltage of 200 kV). X-ray diffraction (XRD) patterns were collected on a Scintag XDS-2000 diffractometer with $Cu_{K\alpha}$ radiation ($\lambda = 1.5406$ Å), with a tube current of 35 mA and a tube voltage of 45 kV. The Au/C and Pt/C catalysts were dissolved in HCl/HNO_3 (3:1, v/v) and the solutions were analyzed by ICP-AES to obtain the catalyst metal loadings.

AEM-DGFC study

The AEM-DGFC tests were performed on a Scribner fuel-cell test system (850e). The fuel-cell fixture was purchased from Fuel Cell Technology Inc. with an active area of 5 cm^2. The end plate was modified with stainless steel (316 L) to tolerate the alkaline working environment. The anode catalyst ink, which was made by mixing a 10 wt% dispersion of PTFE and carbon-supported catalyst powder (Au/C or Pt/C) in water, was sprayed onto a carbon cloth that was used as a liquid diffusion electrode (LDE). The cathode catalyst ink, which was made from a commercial non-platinum-group-metal HYPERMECTM (Fe-Cu-N_4/C, a Fe-Cu-N-based macrocycle that was supported on carbon, Acta) that was blended with an AS-4 anion conductive ionomer (Tokuyama), was spayed directly onto the AEM. 25CC (SGL Group) was applied as the cathode gas-diffusion layer. The membrane electrode assembly (MEA) with an area of 5 cm^2 was fabricated from a mechanically sandwiched anode, an anion-exchange membrane (AEM, Tokuyama A201, 28 μm), and a cathode. A solution of 1.0 M glycerol in 2.0 M KOH was fed into the anode compartment at 4.0 mL min^{-1} and the high-purity O_2 (> 99.999%, 400 mL min^{-1}) was fed into the cathode compartment under a back pressure of 30 psi. The performance of electricity generation from the AEM-DGFC was tested by a polarization scan at 50 or 80 °C. The selective electro-oxidation of glycerol was carried out by looping 2.0 M KOH+1.0 M glycerol (55 mL) from a plastic vessel into the anode plate channels at 50 °C with the same O_2 flow rate (400 mL min^{-1}) and back pressure (30 psi). The oxidation reactions were performed for 2 h by applying various constant voltages. During the reactions, the anode potential was monitored by a Hg/HgO/1.0 M KOH electrode, and reported with respect to an SHE. The generated current density and power density were recorded. Samples were taken after 2 h and analyzed by HPLC.

Electrolysis cell study

The electrocatalytic oxidation of glycerol in an electrolysis cell reactor was performed with two liquid-diffusion electrode (Au-based anode, 5.0 mg_{Au} cm^{-2}, and a Pt-based cathode, 1.0 mg_{Pt} cm^{-2}) and a solid anion-exchange membrane (FAA, 110 μm). The electrolysis cell was assembled as shown in the Supporting Information, Figure S4, with an active cross-sectional area of 1 cm^2 and a Hg/HgO electrode in the anode chamber to control the anode overpotential. The reaction was carried out at each potential for 30 min, with anode electrolyte (1 mL) in the anode chamber and 2.0 M KOH (100 mL) quickly looped into the cathode chamber to remove the H_2 that was generated during the reduction reaction.

Product analysis

The products of the glycerol-oxidation reactions at different potentials were analyzed by using HPLC (Agilent 1100) with a refractive-index detector (RID, Agilent G1326A) and a variable wavelength detector (VWD, 220 nm, Agilent); an OA-1000 column (Alltech) was operated at 60 °C and an eluent of 5 mM aqueous sulfuric acid (0.3 mL min^{-1}) was applied to separation the product. A sample volume of 20 μL was injected into the HPLC system. The products were identified by comparison with authentic samples. The selectivity was calculated according to Equation (1):[3g, 18a]

$$\text{Selectivity} = \frac{\text{Moles of product formed}}{\text{Total moles of } C_2+C_3 \text{ products formed}} \times 100\,\% \quad (1)$$

The carbon balance was based on Equation (2):

$$\text{Carbon balance} = \frac{3M_{Ci}-3M_{C3}-2M_{C2}-M_{C1}-3M_{Cf}}{3M_{Ci}} \times 100\,\% \quad (2)$$

in which M_{Ci} and M_{Cf} are the initial and final moles of glycerol in the electrolyte, and M_{C3}, M_{C2}, and M_{C1} are the moles of the C_3 (glyceric acid, tartronic acid, and mesoxalic acid), C_2 (glycolic acid and oxalic acid), and C_1 products (formic acid and carbonic acid), respectively. If we assumed that no C_2 products were further oxidized into C_1 products, then $M_{C2}=M_{C1}$. Therefore, the carbon balance was given according to Equation (3):

$$\text{Carbon balance} = \frac{M_{Ci}-M_{C3}-M_{C2}-M_{Cf}}{M_{Ci}} \times 100\,\% \quad (3)$$

All of the investigated products were in their deprotonated (salt) forms in alkaline media; herein, we reported them in their acidic forms throughout.

Acknowledgements

We acknowledge the US National Science Foundation (CBET-1032547) for funding and the donors of the American Chemical Society Petroleum Research Fund for partial support of this research. We thank Mr. Ji Qi for his technical support and helpful discussions.

Keywords: fuel cells · glycerol · gold · nanoparticles · oxidation

[1] a) *Breaking the chemical and engineering barriers to lignocellulosic biofuels: next-generation hydrocarbon biorefineries*, **2007**, Workshop report by the NSF, ACS, and US DOE, pp. 1–177; b) G. W. Huber, S. Iborra, A. Corma, *Chem. Rev.* **2006**, *106*, 4044–4098.

[2] a) J. E. H. T. A. Werpy, J. F. White, *Top value added chemicals from biomass: I. Results of screening for potential candidates from sugars and synthesis Gas*, **2004**, US DOE PNNL & NREL Report pp. 52–57; b) C. H. Zhou, J. N. Beltramini, Y. X. Fan, G. Q. Lu, *Chem. Soc. Rev.* **2008**, *37*, 527–549; c) B. Katryniok, H. Kimura, E. Skrzynska, J.-S. Girardon, P. Fongarland, M. Capron, R. Ducoulombier, N. Mimura, S. Paul, F. Dumeignil, *Green Chem.* **2011**, *13*, 1960–1979.

[3] a) P. Gallezot, *Catal. Today* **1997**, *37*, 405–418; b) L. Prati, M. Rossi, *J. Catal.* **1998**, *176*, 552–560; c) S. Carrettin, P. McMorn, P. Johnston, K. Griffin, G. J. Hutchings, *Chem. Commun.* **2002**, 696–697; d) T. Mallat, A. Baiker, *Chem. Rev.* **2004**, *104*, 3037–3058; e) A. Corma, H. Garcia, *Chem. Soc. Rev.* **2008**, *37*, 2096–2126; f) C. Della Pina, E. Falletta, L. Prati, M. Rossi, *Chem. Soc. Rev.* **2008**, *37*, 2077–2095; g) B. N. Zope, D. D. Hibbitts, M. Neurock, R. J. Davis, *Science* **2010**, *330*, 74–78; h) A. S. K. Hashmi, G. J. Hutchings, *Angew. Chem.* **2006**, *118*, 8064–8105; *Angew. Chem. Int. Ed.* **2006**, *45*, 7896–7936; i) M. Pagliaro, R. Ciriminna, H. Kimura, M. Rossi, C. D. Pina, *Angew. Chem.* **2007**, *119*, 4516–4522; *Angew. Chem. Int. Ed.* **2007**, *46*, 4434–4440.

[4] R. Ciriminna, M. Pagliaro, *Adv. Synth. Catal.* **2003**, *345*, 383–388.

[5] a) W. C. Ketchie, Y.-L. Fang, M. S. Wong, M. Murayama, R. J. Davis, *J. Catal.* **2007**, *250*, 94 – 101; b) W. C. Ketchie, M. Murayama, R. J. Davis, *Top. Catal.* **2007**, *44*, 307 – 317; c) S. Carrettin, P. McMorn, P. Johnston, K. Griffin, C. J. Kiely, G. J. Hutchings, *Phys. Chem. Chem. Phys.* **2003**, *5*, 1329 – 1336; d) S. Carrettin, P. McMorn, P. Johnston, K. Griffin, C. J. Kiely, G. A. Attard, G. J. Hutchings, *Top. Catal.* **2004**, *27*, 131 – 136; e) F. Porta, L. Prati, *J. Catal.* **2004**, *224*, 397 – 403; f) C. L. Bianchi, P. Canton, N. Dimitratos, F. Porta, L. Prati, *Catal. Today* **2005**, *102*, 203 – 212; g) N. Dimitratos, C. Messi, F. Porta, L. Prati, A. Villa, *J. Mol. Catal. A* **2006**, *256*, 21 – 28.

[6] Y. Shen, S. Zhang, H. Li, Y. Ren, H. Liu, *Chem. Eur. J.* **2010**, *16*, 7368 – 7371.

[7] a) W. C. Ketchie, M. Murayama, R. J. Davis, *J. Catal.* **2007**, *250*, 264 – 273; b) N. Dimitratos, F. Porta, L. Prati, *Appl. Catal. A* **2005**, *291*, 210 – 214; c) N. Dimitratos, J. A. Lopez-Sanchez, J. M. Anthonykutty, G. Brett, A. F. Carley, R. C. Tiruvalam, A. A. Herzing, C. J. Kiely, D. W. Knight, G. J. Hutchings, *Phys. Chem. Chem. Phys.* **2009**, *11*, 4952 – 4961; d) N. Dimitratos, A. Villa, L. Prati, *Catal. Lett.* **2009**, *133*, 334 – 340; e) D. Wang, A. Villa, F. Porta, L. Prati, D. Su, *J. Phys. Chem. C* **2008**, *112*, 8617 – 8622.

[8] M. Sankar, N. Dimitratos, D. W. Knight, A. F. Carley, R. Tiruvalam, C. J. Kiely, D. Thomas, G. J. Hutchings, *ChemSusChem* **2009**, *2*, 1145 – 1151.

[9] a) M. Simões, S. Baranton, C. Coutanceau, *Appl. Catal. B* **2010**, *93*, 354 – 362; b) J. F. G. G. Tremiliosi-Filho, *Electrocatalysis* **2011**, *2*, 96 – 105; c) D. Z. Jeffery, G. A. Camara, *Electrochem. Commun.* **2010**, *12*, 1129 – 1132.

[10] a) Y. Kwon, K. J. P. Schouten, M. T. M. Koper, *ChemCatChem* **2011**, *3*, 1176 – 1185; b) Y. Kwon, S. C. S. Lai, P. Rodriguez, M. T. M. Koper, *J. Am. Chem. Soc.* **2011**, *133*, 6914 – 6917; c) Y. Kwon, M. T. M. Koper, *Anal. Chem.* **2010**, *82*, 5420 – 5424.

[11] a) E. H. Yu, U. Krewer, K. Scott, *Energies* **2010**, *3*, 1499 – 1528; b) C. Bianchini, P. K. Shen, *Chem. Rev.* **2009**, *109*, 4183 – 4206; c) Z. Zhang, L. Xin, W. Li, *Appl. Catal. B* **2012**, *119 – 120*, 40 – 48; d) A. Ilie, M. Simoes, S. Baranton, C. Coutanceau, S. Martemianov, *J. Power Sources* **2011**, *196*, 4965 – 4971; e) V. Bambagioni, C. Bianchini, A. Marchionni, J. Filippi, F. Vizza, J. Teddy, P. Serp, M. Zhiani, *J. Power Sources* **2009**, *190*, 241 – 251; f) K. Matsuoka, Y. Iriyama, T. Abe, M. Matsuoka, Z. Ogumi, *J. Power Sources* **2005**, *150*, 27 – 31.

[12] a) W. Li, Z. Chen, L. Xu, Y. Yan, *J. Power Sources* **2010**, *195*, 2534 – 2540; b) Z. Zhang, L. Xin, K. Sun, W. Li, *Int. J. Hydrogen Energy* **2011**, *36*, 12686 – 12697; c) Z. Zhang, K. L. More, K. Sun, Z. Wu, W. Li, *Chem. Mater.* **2011**, *23*, 1570 – 1577; d) Z. Zhang, M. Li, Z. Wu, W. Li, *Nanotechnology* **2011**, *22*, 015602.

[13] R. L. Arechederra, S. D. Minteer, *Fuel Cells* **2009**, *9*, 63 – 69.

[14] *Electrocatalysis of Direct Methanol Fuel Cells*, V. B. A. S. Arico, V. Antonucci in *Electrocatalysis of Direct Methanol Fuel Cells*, Wiley-VCH, Weinheim, Germany, **2009**, pp. 1 – 78.

[15] *Knovel Critical Tables*, *2nd ed.*, Knovel, **2003**.

[16] M. Vasiliu, K. Guynn, D. A. Dixon, *J. Phys. Chem. C* **2011**, *115*, 15686 – 15702.

[17] P. Fordham, M. Besson, P. Gallezot, *Catal. Lett.* **1997**, *46*, 195 – 199.

[18] a) B. N. Zope, R. J. Davis, *Top. Catal.* **2009**, *52*, 269 – 277; b) H. Kimura, *J. Polym. Sci. Part A* **1998**, *36*, 195 – 205.

[19] a) S. Demirel, P. Kern, M. Lucas, P. Claus, *Catal. Today* **2007**, *122*, 292 – 300; b) S. Demirel, M. Lucas, J. Warna, D. Murzin, P. Claus, *Top. Catal.* **2007**, *44*, 299 – 305.

[20] P. Fordham, M. Besson, P. Gallezot, *Appl. Catal. A* **1995**, *133*, L179 – L184.

Received: January 11, 2012
Published online on May 22, 2012

